Activity-dependent synaptic GRIP1 accumulation drives synaptic scaling up in response to action potential blockade

Melanie A. Gainey[1,2], Vedakumar Tatavarty[1], Marc Nahmani, Heather Lin, and Gina G. Turrigiano[3]

Department of Biology and Center for Behavioral Genomics, Brandeis University, Waltham, MA 02454

Contributed by Gina G. Turrigiano, June 2, 2015 (sent for review May 1, 2015; reviewed by Serena M. Dudek)

Synaptic scaling is a form of homeostatic plasticity that stabilizes neuronal firing in response to changes in synapse number and strength. Scaling up in response to action-potential blockade is accomplished through increased synaptic accumulation of GluA2-containing AMPA receptors (AMPAR), but the receptor trafficking steps that drive this process remain largely obscure. Here, we show that the AMPAR-binding protein glutamate receptor-interacting protein-1 (GRIP1) is essential for regulated synaptic AMPAR accumulation during scaling up. Synaptic abundance of GRIP1 was enhanced by activity deprivation, directly increasing synaptic GRIP1 abundance through overexpression increased the amplitude of AMPA miniature excitatory postsynaptic currents (mEPSCs), and shRNA-mediated GRIP1 knockdown prevented scaling up of AMPA mEPSCs. Furthermore, knockdown and replace experiments targeting either GRIP1 or GluA2 revealed that scaling up requires the interaction between GRIP1 and GluA2. Finally, GRIP1 synaptic accumulation during scaling up did not require GluA2 binding. Taken together, our data support a model in which activity-dependent trafficking of GRIP1 to synaptic sites drives the forward trafficking and enhanced synaptic accumulation of GluA2-containing AMPAR during synaptic scaling up.

synaptic scaling | synaptic plasticity | GRIP1 | AMPAR | GluA2

Proper development of neuronal circuits, as well as efficient information storage during learning and memory, are thought to depend upon the presence of homeostatic mechanisms that stabilize neuronal excitability (1–3). One such mechanism is synaptic scaling, which compensates for perturbations in average firing by scaling up or down the postsynaptic strength of all of a neuron's excitatory synapses (4). Synaptic scaling is a cell-autonomous process in which neurons detect changes in their own firing through a set of calcium-dependent sensors that then regulate receptor trafficking to increase or decrease the accumulation of AMPA receptors (AMPAR) at synaptic sites and thus increase or decrease synaptic strength (4–6). Despite great recent interest, the AMPA receptor-trafficking events that underlie synaptic scaling remain largely obscure. Defects in synaptic scaling have been postulated to contribute to disorders as diverse as Alzheimer's disease (7) and epilepsy (8), so illuminating the underlying AMPAR trafficking steps could shed light into the genesis of a wide range of neurological disorders.

Most neocortical AMPAR are heteromeric receptors composed of both GluA1 and GluA2 subunits, which have unique phosphorylation sites and interact with distinct trafficking proteins (9). During synaptic scaling up in response to action potential blockade, synaptic strength is increased through enhanced synaptic accumulation of GluA1 and GluA2-containing AMPAR (5, 10–13) and requires the C-terminal domain of the GluA2 subunit (12), but which subunit-specific interactions underlie synaptic scaling remain controversial (12, 14). Several trafficking proteins are known to interact with the GluA2, but not the GluA1, C-tail, including glutamate receptor interacting protein-1 (GRIP1) (15) and protein interacting with C-kinase-1 (PICK1) (16). Many studies have examined the role of GRIP1 and PICK1 in AMPAR trafficking and surface accumulation (15, 17–22), but little is known about their potential roles in regulating AMPAR synaptic accumulation during synaptic scaling. It was recently shown that deletion of PICK1, which competes with GRIP1/2 for binding to GluA2, enhances AMPAR accumulation and occludes synaptic scaling up (23), suggesting GRIP/PICK1-GluA2 interactions as possible critical players in synaptic scaling.

GRIP1 was one of the first AMPAR-binding proteins identified (15), and yet its exact function in synaptic transmission and plasticity remains controversial. GRIP1 is an abundant multi-PDZ domain-containing protein that interacts with GluA2 through its fourth and fifth PDZ domains (15) and has known interactions with several other signaling and trafficking proteins, including itself (24), ABP (25), EphB receptors (26); the rasGEF GRASP-1 (27), the scaffold protein liprin-α (28), and the microtubule motor protein KIF5, or kinesin 1 (29). The role of GRIP1 in AMPAR trafficking is complicated and may involve AMPAR trafficking to and stabilization at synapses (17), as well as microtubule-based transport into dendrites (29) and the regulation of AMPAR movement between intracellular recycling compartments and the cell surface (22, 30). How GRIP1 influences basal AMPAR trafficking is not entirely clear. Overexpression of GRIP1 or gain-of-function GRIP1 mutants have been consistently observed to enhance surface AMPAR levels (21, 31), but knockout or dominant-negative GRIP1 constructs have had inconsistent effects, with slower synaptic AMPAR accumulation

Significance

Brain circuits need plasticity mechanisms that stabilize activity to function properly. Although such homeostatic plasticity mechanisms have been widely described in a number of brain circuits, little is known about the molecular pathways that mediate them. Here, we show that an important form of homeostatic synaptic plasticity at excitatory synapses, synaptic scaling, relies on the activity-dependent accumulation of the glutamate receptor-binding protein glutamate receptor-interacting protein-1 (GRIP1) at synaptic sites. Our data show that GRIP1 is recruited to synapses under conditions of hypoactivity and, through a direct interaction with AMPA-type glutamate receptors, in turn, recruits more AMPA receptors to the synapse. These findings generate molecular insight into the mechanisms that adjust excitatory synaptic strength in response to perturbations in firing.

Author contributions: M.A.G., V.T., M.N., H.L., and G.G.T. designed research; M.A.G., V.T., M.N., and H.L. performed research; M.A.G., V.T., M.N., H.L., and G.G.T. analyzed data; and M.A.G. and G.G.T. wrote the paper.

The authors declare no conflict of interest.

Reviewers included: S.M.D., National Institute of Environmental Health Sciences, National Institutes of Health.

[1]M.A.G. and V.T. contributed equally to this work.

[2]Present address: Department of Molecular and Cellular Biology, University of California, Berkeley CA 94720.

[3]To whom correspondence should be addressed. Email: turrigiano@brandeis.edu.

This article contains supporting information online at www.pnas.org/lookup/suppl/doi:10.1073/pnas.1510754112/-/DCSupplemental.

observed in one study (17) but no effects on basal AMPAR recycling and transmission in others (22, 32). Interestingly, GRIP1 and -2 are critical for the expression of cerebellar long-term depression (LTD), where they play redundant roles in regulated AMPAR endocytosis (33, 34). Currently no direct role for GRIP1 in activity-dependent synaptic strengthening or homeostatic plasticity has been established.

Here, we show that the GRIP1–GluA2 interaction plays an essential role in the activity-dependent synaptic AMPAR accumulation and enhanced excitatory synaptic strength that underlies synaptic scaling up. Activity blockade with TTX increased the accumulation of GRIP1 at synaptic sites, whereas directly enhancing synaptic GRIP1 accumulation through overexpression (OE) was sufficient to mimic synaptic scaling. GRIP1 was necessary for synaptic scaling, because scaling up was prevented by shRNA-mediated knock down (KD) of endogenous GRIP1 and rescued by replacement with an RNAi-insensitive (RNAiI) GRIP1 but not a GRIP1 mutant that lacks the GluA2 interaction domain. We showed previously that GluA2 KD blocks synaptic scaling (12). Here, we show that synaptic scaling after GluA2 KD can be rescued by wild-type (RNAiI) GluA2 or point mutants that do not interfere with GRIP1 binding but not by GluA2 point mutants (Y876E and S880E) that reduce GluA2- GRIP1 binding, strongly suggesting that GRIP1 mediates synaptic scaling through interactions with GluA2. Finally, TTX still induced GRIP1 synaptic accumulation even when AMPAR accumulation was prevented by expression of GluA2 Y876E; thus, during synaptic scaling GluA2 synaptic accumulation depends on GRIP1 binding, but GRIP1 translocation and synaptic accumulation occur independently of GluA2 binding. Together our data show that activity-dependent regulation of synaptic GRIP1 abundance is critical for the forward trafficking and accumulation of AMPA receptors at synapses during synaptic scaling.

Results

We showed previously that the GluA2 C-tail is required for TTX-induced synaptic scaling up (12). Here, we wished to determine the role of the GluA2 C-tail binding protein, GRIP1, in synaptic scaling. Experiments were performed on cultured postnatal rat visual cortical neurons on 7–10 d in vitro (DIV). Synaptic scaling was induced with a 6-h TTX treatment as

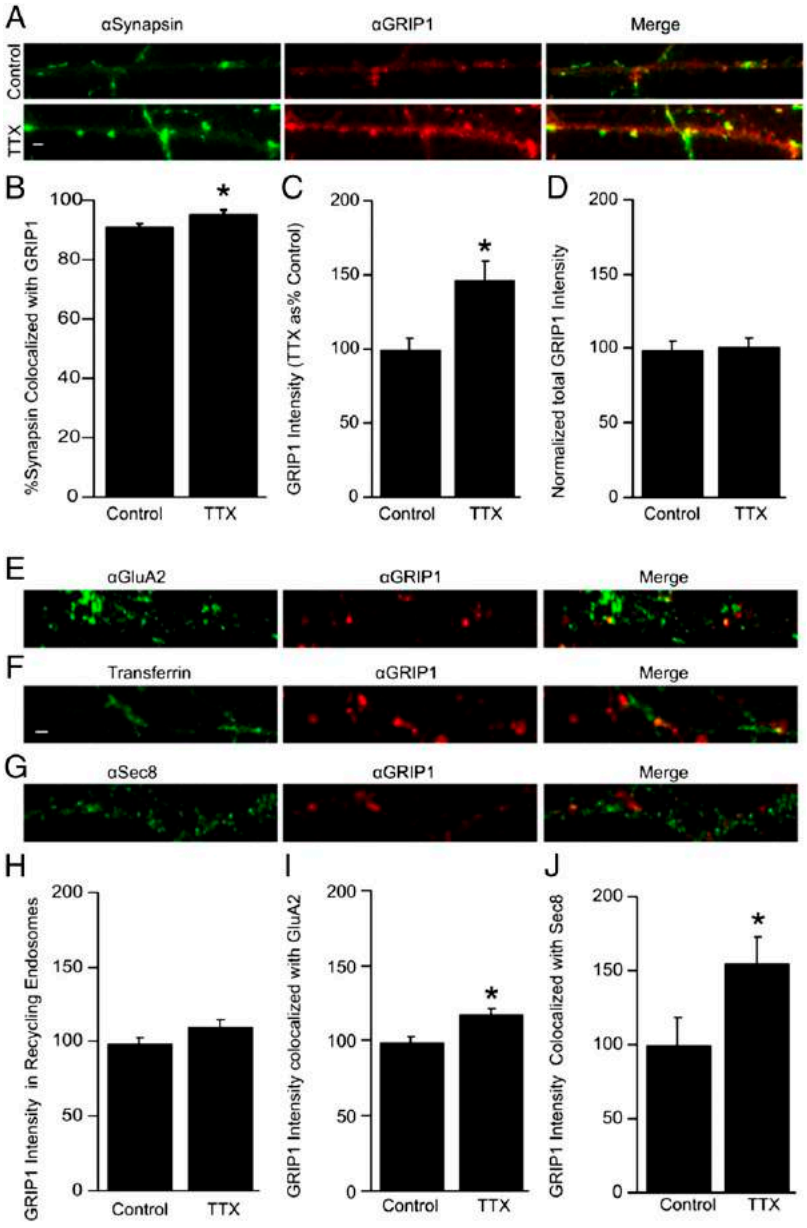

Fig. 1. Activity blockade drives increased synaptic GRIP1 accumulation. (*A*) Examples of staining against synapsin (green) and GRIP1 (red) in control (top images) (upper images) and 6-h TTX conditions (lower images). (*B*) Percentage of synapsin puncta colocalized with GRIP1 puncta in control and TTX conditions. (*C*) Average Intensity of GRIP1 puncta that colocalized with synapsin; values from TTX-treated neurons expressed as percentage of untreated controls. (*D*) Analysis of the total GRIP1 dendritic signal (normalized to dendritic area) for control and TTX conditions; values from TTX-treated neurons expressed as percent of untreated controls. (*E*, *F*,and *G*) Example dendritic images showing colabeling against GRIP1 and GluA2 (*Top*), transferrin (*Middle*), or sec8 (*Bottom*), respectively. (*H*, *I*, and *J*) Intensity of the GRIP1 signal at puncta that colocalize with Transferrin (*H*), GluA2 (*I*), or Sec8 (*J*); values from TTX-treated neurons expressed as percentage of untreated control. (Scale bar: 1 μm.) *Different from control, $P < 0.05$. Here and below, all *n* values are given in the results section, and all data are presented as means ± SEM for the number of neurons (*n*) indicated.

described (5, 35). Neurons were transfected at low efficiency with various constructs for 2 d before recording or immunolabeling. Whole-cell recordings and images were obtained from pyramidal neurons identified morphologically as described (36).

Activity Blockade Increases the Synaptic Accumulation of GRIP1. We began by asking whether GRIP1 synaptic localization and/or abundance are regulated by activity blockade. First, we verified the specificity of our GRIP1 antibodies (mouse and rabbit) for immunohistochemistry by transfecting neurons with HA- or GFP-tagged GRIP1 and quantifying colocalization between the GRIP1 and the αGRIP1 signals; dendritic line scans indicate that the signals covary almost perfectly (Fig. S1*A*), and there was >90% colocalization between puncta (Fig. S1 *B* and *C*). Previous studies have shown that GRIP1 has a broad spatial distribution in neurons with localization to axons, excitatory and inhibitory synapses, and intracellular membranes (15, 37); consistent with this finding, we found that although most presynaptic sites (labeled with synapsin) are apposed to GRIP1 puncta (~91%; Fig. 1 *A* and *B*), the majority of GRIP1 puncta were extrasynaptic (only 14.6% of GRIP1 puncta colocalized with synapsin). After 6 h of TTX treatment, there was a small but significant increase in the percentage of synapsin puncta colocalized with GRIP1 (Fig. 1*B*; control: $n = 10$ neurons, TTX: $n = 17$ neurons; $P < 0.05$). Furthermore, the intensity of the punctate GRIP1 signal was significantly enhanced at these putative synaptic sites (Fig. 1 *A* and *C*). To differentiate between a redistribution of GRIP1 to putative synaptic sites versus a general increase in GRIP1 protein, we quantified the total dendritic GRIP1 signal (normalized for dendritic area) and found no significant change following TTX treatment (Fig. 1*D*).

Because GRIP1 is widely distributed at both synaptic and nonsynaptic sites, we next used markers of different endosomal compartments to ask where (in addition to synaptic sites) GRIP1 accumulates during TTX treatment. We labeled against GRIP1 and either GluA2 (Fig. 1*E*), a marker against recycling endosomes (Transferrin; Fig. 1*F*), or a component of the exocyst complex (Sec8; Fig. 1*G*) and determined the intensity of the colocalized GRIP1 signal with or without TTX treatment. As expected, a subset of GRIP1 puncta (18.8% and 9.0% respectively) colocalized with a subset of TfR- or Sec8-positive puncta; TTX did not significantly affect these colocalization rates. TTX had no significant effect on the intensity of the GRIP1 signal colocalized with transferrin (Fig. 1 *F* and *H*; control, $n = 83$; TTX, $n = 91$) but did significantly increase GRIP1 accumulation at sites colocalized with GluA2 (Fig. 1 *E* and *I*) and Sec8 (Fig. 1 *G* and *J*; control, $n = 71$; TTX, $n = 73$). As a control, we verified that the actual rate of GRIP1/Sec8 colocalization is significantly higher than expected if the distribution of Sec8 were random relative to GRIP1 (see methods and Fig. S2).

Synaptic scaling of AMPA miniature excitatory postsynaptic currents (mEPSCs) and the underlying accumulation of synaptic GluA2 are known to be transcription-dependent (5). Consistent with this, the transcriptional inhibitor actinomycin D (ActD) prevented the TTX -induced increase in punctate GluA2 signal (Fig. S3*A*) and also prevented the accumulation of GRIP1 at sites colocalized with GluA2 (Fig. S3*B*). TTX induced no significant change in the dendritic length density of GRIP1 puncta ($P = 0.38$). Taken together with the observation that TTX does not affect total dendritic GRIP1 protein (Fig. 1*D*), these data suggest that activity blockade induces a transcription-dependent translocation of GRIP1 to synaptic sites, as well as to other select endosomal compartments.

Finally, to determine whether TTX increases GRIP1 specifically at the postsynaptic density (rather than, for example, perisynaptically), we did postembedding immuno-EM on cultured synapses (Fig. 2). Excitatory synapses onto pyramidal neurons were labeled presynaptically against VGluT1 [Fig. 2 *A* and *B*, dark diaminobenzidine (DAB) signal] and GRIP1 (Fig. 2 *A* and *B*, gold particles). As described previously (37), GRIP1 was localized in both the presynaptic and postsynaptic compartments. There was clear accumulation of GRIP1 at the postsynaptic density, as well as in membrane-bound compartments within the synapse (Fig. 2*B*). An analysis of the distribution of gold particles showed the highest levels at the synaptic cleft, with a steep drop-off to either side. At TTX-treated synapses, the density of GRIP1 labeling was significantly higher in the postsynaptic compartment, with the largest increase close to the postsynaptic density (Fig. 2*C*; control, $n = 42$ synapses; TTX, $n = 37$ synapses). Quantification of the density of gold particles within 40 nm of the synaptic cleft showed a significant increase following TTX treatment (Fig. 2*D*). These data raise the possibility that GRIP1

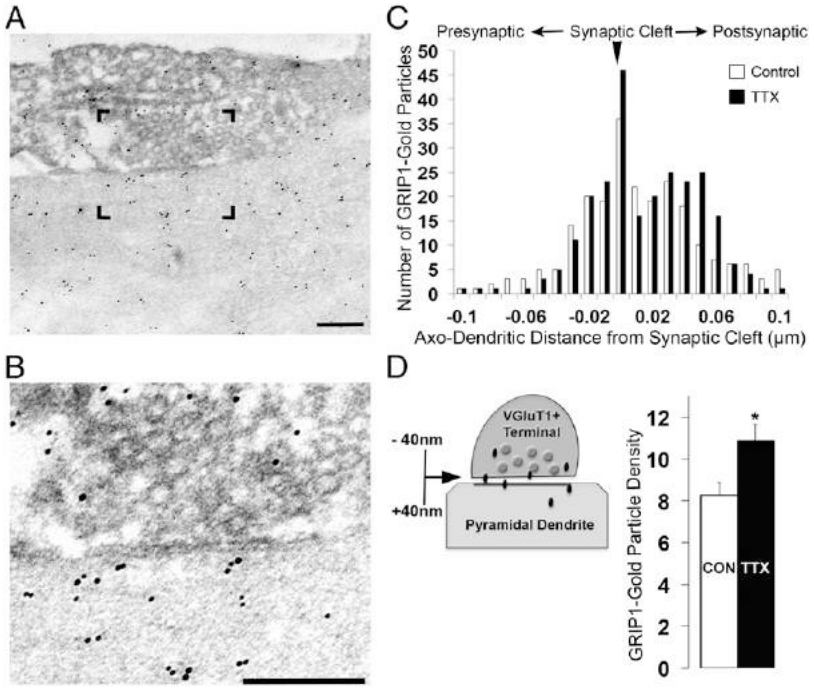

Fig. 2. (*A*) Electron micrograph showing a vesicle-filled VGluT1$^+$ presynaptic bouton (dark DAB labeling) with a synapse onto a cultured pyramidal neuron dendrite. This section was also stained with an anti-GRIP1 antibody coupled to a 5-nm gold secondary (gold particles). Black corners mark cropped image shown in *B*. Note the abundant gold particles adjacent to the synapse. (*B*) Enlarged area of image shown in *A*, showing apposition of GRIP1-gold particles with postsynaptic membrane. (*C*) Distribution of presynaptic (negative values) and postsynaptic (positive values) GRIP1-gold particles along the axodendritic axis at VGluT1$^+$/pyramidal cell synapses. Note that the peak in the GRIP1-gold distribution is centered at the synaptic cleft for both control (white) and TTX (black) condition. (*D*) Synaptic GRIP1-gold density, defined as ±40nm in axodendritic distance from the synaptic cleft (to account for antibody linkage distance), for control and TTX conditions. *$P < 0.02$, Mann–Whitney *U* test. (Scale bars: 200 nm for *A* and *B*.)

plays a role in trafficking GluA2 to synapses during synaptic scaling.

Overexpression of GRIP1 Is Sufficient to Increase mEPSC Amplitude. Because GRIP1 accumulates at synapses during activity blockade, we next asked whether directly increasing GRIP1 levels through OE was sufficient to drive more GRIP1 to synapses and to increase mEPSC amplitude. OE of GRIP1 for 2 d significantly enhanced the intensity of the GRIP1 signal at puncta that colocalize with postsynaptic density-95 (PSD-95) (Fig. 3 *A* and *B*; control, $n = 10$; GRIP1 OE, $n = 9$; $P < 0.01$). Furthermore, baseline mEPSC amplitude (but not frequency) was significantly increased in GRIP1 OE neurons compared with control (Fig. 3 *C–E*; control, $n = 8$; GRIP1 OE, $n = 7$; mEPSC amplitude in the GRIP1 OE condition was 141.2 ± 19% of control; $P < 0.05$). Together, these results indicate that OE of GRIP1 is sufficient to increase the accumulation of GRIP1 at synaptic sites and to drive an increase in AMPA mEPSC amplitude.

GRIP1 Is Necessary for the Expression of Synaptic Scaling Up. The data described above suggest that activity blockade induces synaptic scaling by enhancing the synaptic accumulation of GRIP1. If so, then reducing neuronal GRIP1 should attenuate or abolish synaptic scaling. GRIP1 KO is embryonic lethal (38, 39), so to reduce GRIP1 levels acutely and in a cell-autonomous manner, we used an shRNA against GRIP1 (40) to selectively KD GRIP1 in individual cultured cortical pyramidal neurons. A 2-d expression of the GRIP1 shRNA (KD) reduced GRIP1 puncta intensity to 46% of control and also produced a 37% reduction in dendritic length density of GRIP1 puncta (Fig. 4 *A* and *B*; control, $n = 14$ neurons; GRIP1 KD, $n = 13$ neurons), giving a total KD to ~35% of control levels. This degree of KD was sufficient to completely block synaptic scaling; a 6-h treatment with TTX significantly enhanced mEPSC amplitude in control neurons as described previously (5, 35) but not in GRIP1 KD neurons (Fig. 4 *C* and *D*; control, $n = 46$; TTX, $n = 55$; TTX was 129.6 ± 7.3% of control; $P < 0.0001$; control GRIP1 KD, $n = 13$; TTX GRIP1 KD, $n = 8$; TTX was 103.8 ± 10.8% of control; $P = 0.73$).

To control for any potential off-target effects of the hairpin, we cotransfected neurons with the GRIP1 shRNA and an RNAi-resistant GRIP1 construct (Rescue) and asked whether we could rescue synaptic scaling. Indeed, scaling was normal in neurons transfected with the shRNA and the rescue construct (Fig. 4 *C* and *D*; control GRIP1KD & Rescue, $n = 13$; TTX GRIP1KD & Rescue, $n = 11$; TTX was 132.5 ± 12.9% of control; $P < 0.01$). GRIP1 interacts with GluA2 through PDZ domains 4–5 (9); a mutated form of RNAiI GRIP1 missing PDZ domains 4–6 (40) was unable to rescue scaling (Fig. 4*D*). These data demonstrate that GRIP1 is essential for synaptic scaling up, and raise the possibility that scaling may require a direct interaction between GRIP1 and GluA2.

Manipulating GRIP1 Expression Does Not Affect mEPSC Kinetics or Passive Properties. Longer KD of GRIP1 (4 d) has been reported to impact dendritic elaboration in cultured hippocampal neurons (40), raising the possibility that changes in electrotonic filtering could contribute to the changes in mEPSC amplitude we observe upon manipulations of GRIP1 levels. To address this possibility, we measured the mEPSC kinetics, and the passive properties of neurons, upon OE or KD of GRIP1. Neither OE nor KD of GRIP1 had any significant effect on mEPSC rise time or decay (Fig. 5*A*: control, $n = 8$; GRIP1 OE, $n = 7$; for rise, $P = 0.25$; for decay, $P = 0.31$; Fig. 5*B*: control, $n = 5$; GRIP1 KD, $n = 13$; for rise, $P = 0.59$; for decay, $P = 0.46$). Thus, changes in mEPSC amplitude are independent of changes in electrotonic filtering.

In addition, dendritic morphologies appeared normal in OE and KD neurons, and these manipulations had no significant impact on whole cell capacitance or input resistance (Fig. 5*C*;

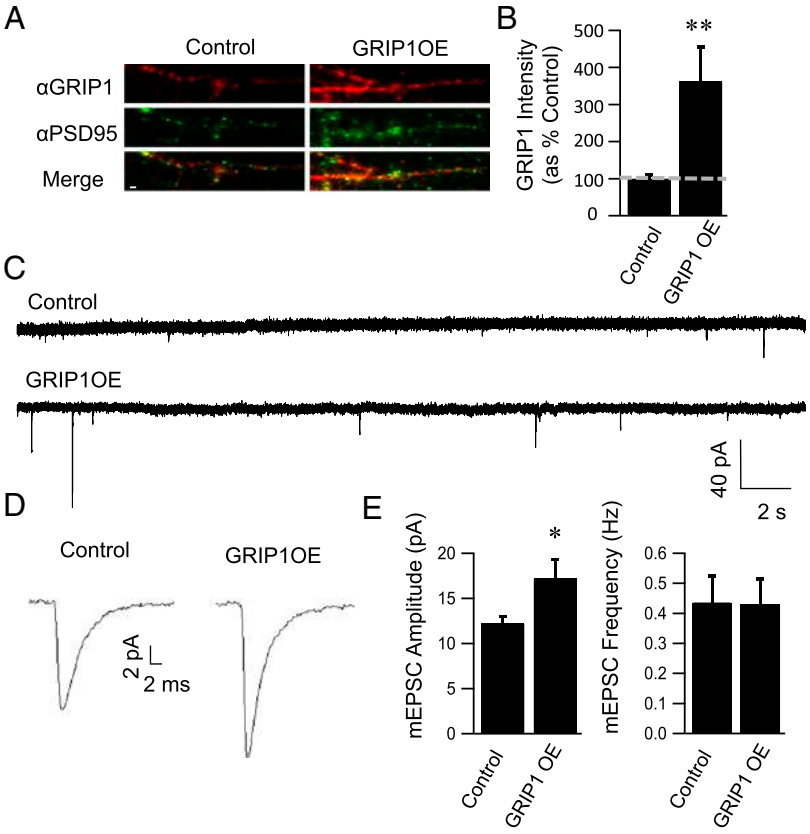

Fig. 3. Overexpression of GRIP1 increases synaptic GRIP1 accumulation and mEPSC amplitude. (*A*) Example of control (*Left*) and GRIP1 OE (*Right*) dendrites labeled against PSD-95 (in green) and GRIP1 (in red; endogenous in control, both endogenous and exogenous in GRIP1 OE condition). (Scale bar: 1 μm.) (*B*) Average Intensity of GRIP1 puncta colocalized with PSD-95 for control and GRIP1 OE conditions; values from GRIP1 OE neurons expressed as percentage of control neurons. (*C*) Example mEPSC recordings from control and GRIP1OE neurons. (*D* and *E*) Average mEPSC waveform (*D*) and average mEPSC amplitude (*E*) (*Left*) and frequency (*Right*) for control and GRIP1 OE conditions. *Different from control, $P < 0.05$, **$P < 0.01$.

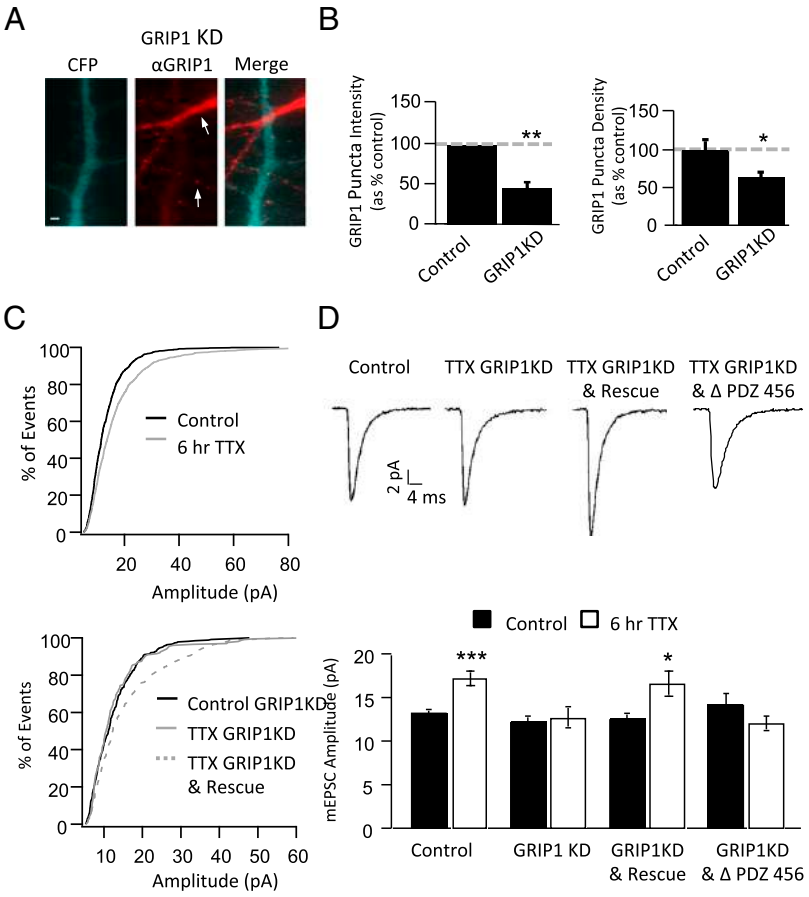

Fig. 4. GRIP1 KD blocks synaptic scaling. (*A*) Sparse transfection of cultured neurons with the GRIP1 shRNA and soluble CFP (blue) (to label transfected neurons and dendrites) and αGRIP1 (red); the dendrite from the hairpin-expressing neuron shows little GRIP1 signal relative to the nontransfected dendrite (arrows). (*B*) Puncta Intensity (*Left*) and length density (puncta per μm) (*Right*) of GRIP1 puncta for control or shRNA-transfected dendrites; values from GRIP1KD neurons expressed as percentage of control. (*C*) Cumulative histograms of mEPSC amplitude from neurons in control and TTX conditions (*Upper*) and control GRIP1KD, TTX GRIP1KD, and TTX GRIP1KD & Rescue (*Lower*). (*D*) Average mEPSC waveform (*Upper*) and average mEPSC amplitudes from indicated conditions (*Lower*). (Scale bar: 1 μm.) *Different from control: $P < 0.05$; **$P < 0.001$.

ANOVA, $P = 0.58$ for capacitance and $P = 0.39$ for input resistance), together suggesting that cell size and overall dendritic branching is unperturbed by a two day manipulation of GRIP1 expression. Thus, it is unlikely that the failure to scale in GRIP1KD neurons is a secondary effect of changes in dendritic morphology.

Expression of Synaptic Scaling Requires Association Between GluA2 and GRIP1. Next, we wished to determine whether direct interactions between GRIP1 and GluA2 are required for the expression of synaptic scaling. To address this possibility, we used site-directed mutagenesis to create four GluA2 C-tail phosphorylation mutants that either disrupt binding between GluA2 and GRIP1 (Y876E, S880E) or leave GRIP1/GluA2 binding unaffected (Y876F, K882A). The S880E mutant is a phosphomimetic mutation known to reduce the interaction between GluA2 and GRIP1 (32, 41, 42). It has been shown that phosphorylation of tyrosine 876 after glutamate stimulation causes a reduced interaction between GluA2 and GRIP1 in cultured neurons (43), so we designed a second phosphomimetic mutation for the tyrosine 876 residue (Y876E) as a second means of reducing GRIP1/GluA2 binding. The Y876F mutation renders tyrosine 876 nonphosphorylatable and does not affect binding between GluA2 and GRIP1 (43). The K882A mutant blocks phosphorylation of serine 880 by protein kinase C (PKC) and also does not perturb binding between GluA2 and GRIP1 (41).

We have previously shown that synaptic scaling is blocked by GluA2 KD and rescued by coexpression of an RNAi-resistant WT GluA2 subunit (12). Here, we use this KD and replace strategy to determine which of the GluA2 phosphorylation mutants are able to rescue synaptic scaling. Neurons were cotransfected with the GluA2 shRNA (GluA2KD) and various GluA2 subunits resistant to the hairpin for 2 d and then treated with TTX for 6 h to induce synaptic scaling. In control neurons, 6 h of TTX significantly enhanced mEPSC amplitude (Figs. 4*C* and 6*B*; control, $n = 46$; TTX, $n = 55$; $P < 0.0001$). On a GluA2 KD background, the two phosphomimetic GluA2 mutants with reduced GRIP1 binding, Y876E and S880E failed to rescue scaling (Fig. 6 *A* and *B*; Y876E: control, $n = 8$; TTX, $n = 8$; $P = 0.7$; S880E: control, $n = 8$; TTX, $n = 8$; $P = 0.75$). In contrast, the two nonphosphorylatable mutants that do not disrupt GRIP binding, Y876F and K882A, were able to rescue scaling (Fig. 6 *A* and *B*; Y876F: control, $n = 12$; TTX, $n = 9$; $P < 0.05$; K882A: control, $n = 6$; TTX, $n = 8$; $P < 0.05$). Together, these data suggest that the interaction between GluA2 and GRIP1 is required for the expression of synaptic scaling. Because there is some evidence that GRIP1 is important for basal trafficking of AMPA receptors (21, 32, 44), we also examined whether the GluA2 mutants on a GluA2 KD background affected the baseline amplitude of mEPSCs. None of these mutations on a GluA2KD background induced any significant change in mEPSC amplitude compared with nontransfected neurons, suggesting that basal trafficking is unperturbed (Fig. 6*C*; ANOVA $P = 0.98$).

The failure of Y876E and S880E to rescue synaptic scaling could be explained by a defect in the targeting of these subunits to synaptic membranes. To confirm that the mutant GluA2 subunits are able to traffic to synapses, we performed live cell immunolabeling against a GFP tag in the extracellular N-terminal domain under nonpermeable conditions, fixed, and then counterstained against the postsynaptic marker PSD-95. All of the mutant GluA2 subunits on a GluA2 KD background colocalized with PSD-95 to a similar extent as the wild-type RNAiI rescue construct (GluA2) (Fig. 6 *D*; $n = 6$ neurons per condition; ANOVA, $P = 0.46$). Furthermore, the intensity of the surface GFP signal at synaptic sites was not significantly different between these various mutants (Fig. S4), indicating that the failure

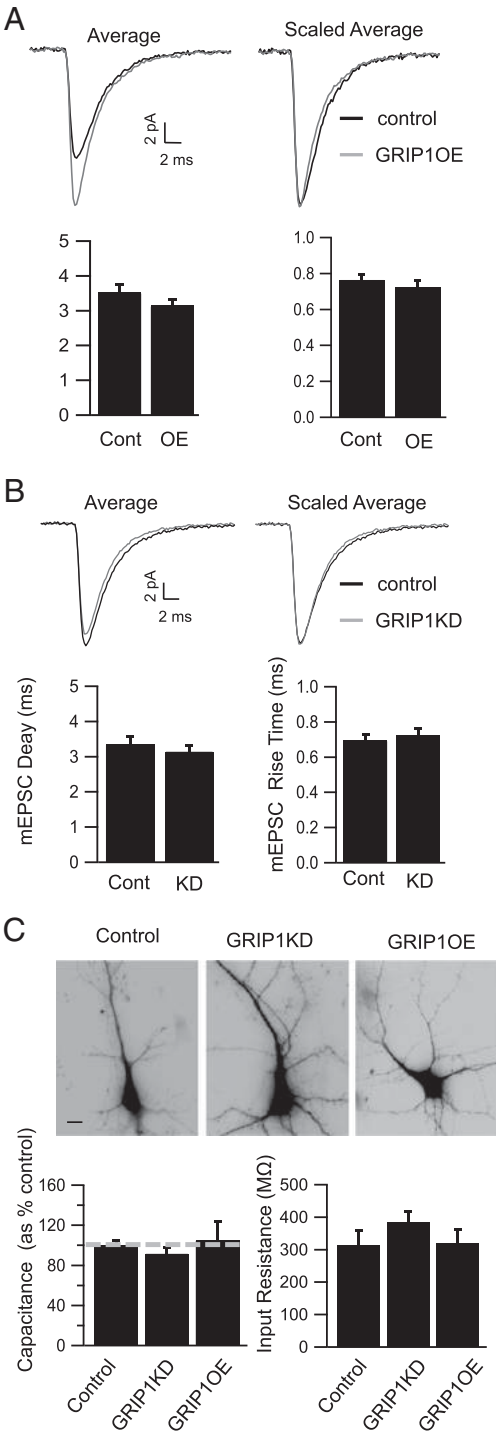

Fig. 5. Manipulations of GRIP1 do not affect mEPSC kinetics or passive neuronal properties. (*A*) Average mEPSC waveforms (*Left*) and peak-scaled waveforms (*Right*) (to allow comparison of kinetics) from control and GRIP1 OE neurons (*Upper*) and average mEPSC decay tau and rise times for the indicated conditions (*Lower*). (*B*) Average mEPSC waveforms (*Left*) and peak-scaled waveforms (*Right*) from control and GRIP1KD neurons (*Upper*) and average mEPSC decay tau and rise times for the indicated conditions (*Lower*). (*C*) Representative images of dendritic morphology for control, GRIP1KD, and GRIP1OE neurons (*Upper*) and whole-cell passive properties for indicated conditions (*Lower*). (Scale bar: 10 μm.)

of Y876E and S880E to rescue scaling is not attributable to general (basal) trafficking defects but rather to blockade of a regulated interaction between GluA2 and GRIP1 that is necessary for scaling up.

Activity Blockade Leads to Synaptic GRIP1 Accumulation Independently of GluA2. Taken together, our data show that synaptic scaling up depends upon the interaction between GluA2 and GRIP1. This raises the question of whether enhanced GRIP1 accumulation at synapses drives the increase in synaptic GluA2, or vice versa. To address this question, we first asked whether we could block synaptic scaling by using the GluA2 Y876E as a dominant negative. Similar to the effects of Y876E expression on a GluA2 KD background (Fig. 6 *A* and *B*), synaptic scaling was completely blocked by expression of the Y876E construct alone (Fig. 7*A*; control, $n = 7$; TTX, $n = 6$; $P = 0.93$). Next, we prevented the expression of synaptic scaling by transfecting neurons with the GluA2 Y876E mutant and asked whether GRIP1 still accumulates at synapses when neurons are treated with TTX for 6 h. Neurons were immunolabeled against GRIP1 and PSD-95 and the intensity of the synaptic GRIP1 signal quantified. Consistent with our earlier observations (Figs. 1 and 2), 6 h of TTX caused a significant increase in the intensity of GRIP1 puncta colocalized with PSD-95 (Fig. 7B; control, $n = 25$ neurons; TTX, $n = 10$ neurons; $P < 0.05$). Interestingly, GRIP1 accumulation at synaptic sites was normal in Y876E-expressing neurons (Fig. 7*B*; control, $n = 14$; TTX, $n = 10$; $P < 0.05$), suggesting that GRIP1 is able to traffic to synapses in an activity-dependent manner independently of GluA2. These data support a model in which activity-dependent trafficking of GRIP1 to synapses drives the accumulation of GluA2 during synaptic scaling.

Discussion

Synaptic scaling is a form of homeostatic plasticity that adjusts the weights of all of a neuron's synapses in proportion to their initial strength (4). During TTX-induced synaptic scaling up, synapses are strengthened through increased synaptic accumulation of GluA1 and GluA2-containing AMPA receptors (11), in a manner that requires the GluA2, but not the GluA1, C-tail (12). Despite much recent interest in the mechanisms of synaptic scaling, the GluA2-dependent receptor trafficking steps that underlie scaling up remain largely undefined. Here, we examine the possibility that synaptic scaling requires GluA2 interactions with GRIP1, a multi-PDZ domain-containing trafficking/scaffolding protein that binds the GluA2, but not the GluA1, C-tail (15). Although GRIP1 was one of the first AMPAR binding proteins to be identified, its precise role in AMPAR trafficking is still unclear, and whether it is important for homeostatic plasticity is completely unexplored. Here, we provide several lines of evidence that activity-dependent increases in synaptic GRIP1 are necessary for the induction of synaptic scaling up. We find that synaptic GRIP1 levels increase during activity blockade and that directly enhancing synaptic GRIP1 increases mEPSC amplitude. Furthermore, GRIP1 KD prevents synaptic scaling up, and both the inactivity-induced increase in mEPSC amplitude and in GluA2 trafficking require the GluA2-GRIP1 interaction. Together, our results support a model in which activity-dependent trafficking of GRIP1 to synaptic sites drives the forward trafficking and enhanced accumulation of GluA2-containing AMPAR during synaptic scaling.

GRIP1 is an abundant protein that has been strongly implicated in the transport and synaptic maintenance of GluA2-containing AMPAR, but contradictions in the literature have led to uncertainly about its precise role. GluA2 point mutants that fail to bind GRIP1 show decreased synaptic accumulation in some studies (17, 32) but not in another (19). GluA2 has reduced surface expression on a GRIP1 dominant-negative background (31) but, consistent with our data, shows normal surface expression on a GRIP knockout background (22). We found that acute KD of GRIP1, as well as replacement of GluA2 with point mutations that have decreased binding to GRIP1, do not significantly affect baseline mEPSC amplitude or frequency. Furthermore, GluA2 point mutants with reduced GRIP1 binding

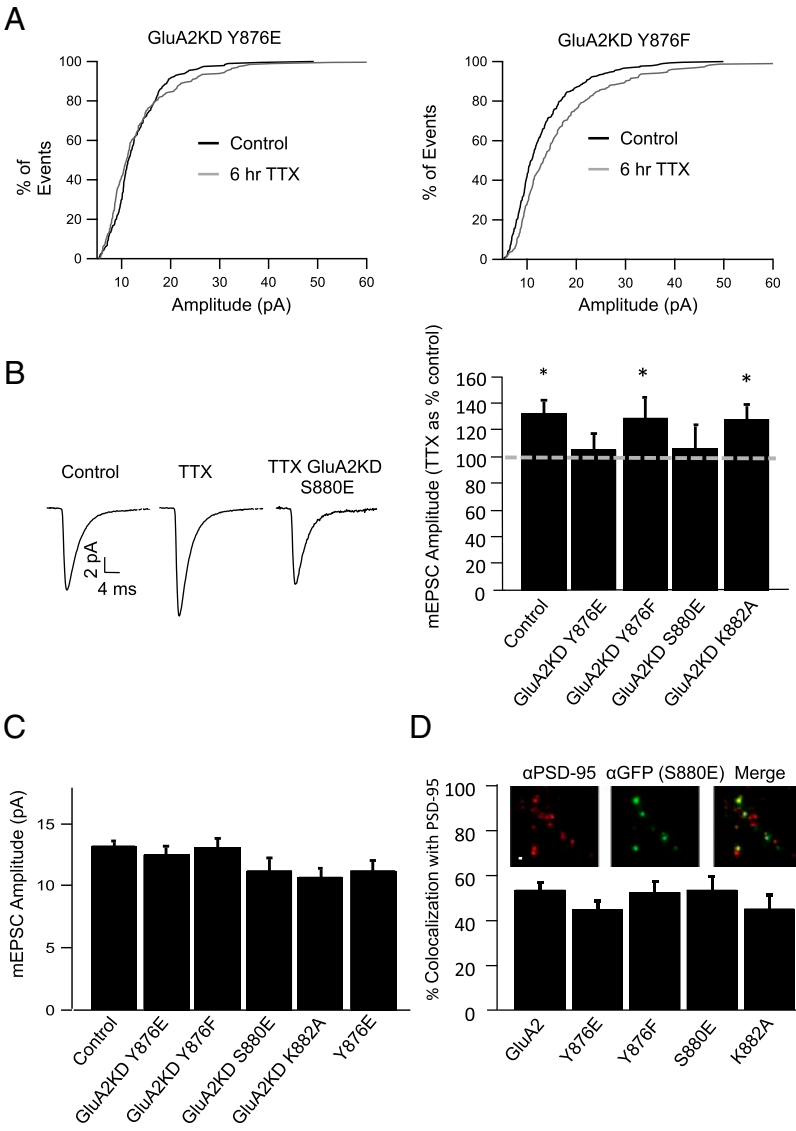

Fig. 6. Interaction between GluA2 and GRIP1 is required for synaptic scaling. (*A*) Cumulative histograms of mEPSC amplitude showing effects on scaling of KD and replace of GluA2 with point mutants: Y876E (*Left*) and Y876F (*Right*) for the control and TTX conditions. (*B*) Average mEPSC waveforms (*Left*) and average mEPSC amplitudes for indicated conditions (*Right*); TTX is expressed as percentage of control for the same condition. (*C*) Average control mEPSC amplitudes for indicated conditions. (*D*) Synaptic localization of GluA2 constructs, imaged using extracellular GFP tag. Average colocalization rates of indicated GluA2 subunits with PSD-95 on a GluA2KD background (*Lower*) and example GluA2KD S880E dendrites labeled against GFP (green) under nonpermeable conditions to localize surface GluA2 and counterstained against PSD-95 (red) (*Upper*). (Scale bar: 1 μm.) *Different from control, $P < 0.05$.

show normal mEPSC amplitudes and localization to synaptic sites, suggesting that basal targeting of AMPAR to synapses is unimpaired. Together, our data strongly suggest that GRIP1 is not required for normal constitutive trafficking of AMPARs in our young neocortical neurons but rather plays a specific role in the regulated accumulation of GluA2 that underlies synaptic scaling up.

In addition to binding GRIP1, the GluA2 CT also binds the PDZ domain-containing protein PICK1. PICK1 competes with GRIP1 for binding to the same region of the GluA2 C-tail, in a manner regulated by GluA2 phosphorylation (32). In general, GRIP1 and PICK1 are thought to have opposing roles in AMPAR trafficking, with GRIP1 promoting forward trafficking of GluA2-containing AMPA receptors to synapses (15, 17, 21, 22, 32) and PICK1 triggering internalization (23, 33, 45). Phosphorylation of GluA2 on amino acids 876 by the tyrosine kinase lyn (43) or 880 by PKC (32) blocks GRIP1 binding but leaves PICK1 binding unperturbed. A recent study showed that PICK1 levels are activity-regulated in a manner opposite to what we show here for GRIP1; chronic activity blockade reduces PICK1 (23) at the same time that it increases GRIP1 (Fig. 1). Furthermore, AMPA receptor accumulation is enhanced and synaptic scaling up occluded by PICK1 knockout (23). Because GRIP1 and PICK1 compete for GluA2 binding, knockout of PICK1 should enhance GRIP1 binding to AMPAR; GRIP1 OE should do much the same thing by outcompeting PICK1, and both of these manipulations lead to enhanced synaptic AMPAR accumulation and increased mEPSC amplitude (ref. 23 and Fig. 3). These observations suggest that reciprocal activity-dependent regulation of GRIP1 and PICK1 cooperate to induce synaptic scaling up in response to inactivity.

GRIP1 is required for normal synaptic scaling, because acute KD of GRIP1 leaves baseline transmission intact but blocks synaptic scaling up. Furthermore, synaptic scaling was critically dependent on the GluA2 -GRIP1 interaction, because GRIP1 PDZ mutants that cannot bind GluA2 fail to rescue scaling on a GRIP1 KD background, whereas phosphomimetic GluA2 point mutants with reduced binding to GRIP1 failed to rescue synaptic scaling on a GluA2 KD background. Because all of these GluA2 mutants showed normal localization to synapses and normal baseline mEPSC amplitudes, these differences cannot be attributed to failure to constitutively traffic to synapses but rather must result from a failure of regulated trafficking during scaling up. Interestingly, the GluA2 Y876E point mutant can also be used as a dominant negative to block synaptic scaling, suggesting that GluA2 Y876E largely replaces endogenous GluA2 when overexpressed.

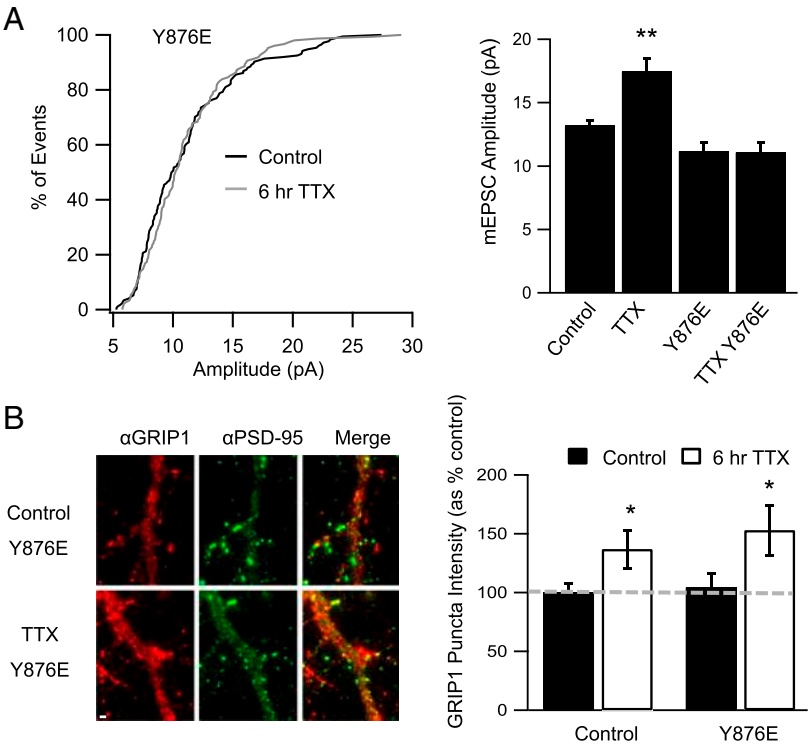

Fig. 7. Chronic inactivity induces synaptic GRIP1 accumulation independently of GluA2 binding. (*A*) Cumulative histogram of mEPSC amplitude in Y876E neurons in control and TTX conditions (*Left*) and average mEPSC amplitude for indicated conditions (*Right*). (*B*, *Left*) Example of Y876E-expressing neurons in control (*Upper*) and TTX (*Lower*) conditions, labeled against GRIP1 (red) and PSD-95 (green). (Scale bar: 1 μm.) (*B*, *Right*) Average intensity of GRIP1 puncta colocalized with PSD-95, for control or Y876E-expressing neurons; TTX expressed as percentage of control for same condition. *Different from control: $P < 0.05$; **$P < 0.001$.

Our data currently cannot distinguish between a role for GRIP1 in the forward trafficking of GluA2 to synaptic membranes from intracellular compartments or as an anchoring protein for GluA2 at synaptic sites during synaptic scaling. There is evidence that GRIP1 is required for transporting internalized AMPARs to the cell surface in an activity-dependent manner, through association with NEEP21 (30) and Sec8 (22). Sec8 is a member of the exocyst complex important for vesicle fusion and is localized to a number of endosomal compartments as well as to sites of exocytosis on the plasma membrane (46). We find that TTX treatment increases GRIP1 accumulation at Sec8-positive internal sites as well as at the postsynaptic density. This raises the interesting possibility that GRIP1 might be important for the forward trafficking of AMPAR to exocytotic sites during scaling up. The increased accumulation of GRIP1 at synaptic sites suggests that GRIP1 remains associated with AMPAR after they reach the synaptic membrane, where GRIP1 could play an additional role in the stabilization of the receptors. Although mutations that prevented GluA2 from interacting with GRIP1 prevented the enhanced trafficking of GluA2 to synapses, TTX still drove GRIP1 to synaptic sites under these conditions. These data strongly suggest that, during synaptic scaling, movement of GRIP1 to synapses drives the enhanced accumulation of GluA2 rather than the other way around.

This study demonstrates that GRIP1 localization can be regulated by activity, but how this regulation is accomplished is not clear. GRIP1 can be multiply phosphorylated by PKC and other kinases (47), and AMPA or NMDA stimulation enhances the phosphorylation of GRIP1, which affects the binding of GRIP1 to NEEP21 and thus modifies the endosomal sorting of GluA2 (31), but the endogenous kinase(s) responsible for GRIP1 phosphorylation, and the signals that normally activate them, are unknown. Interestingly, we found that total dendritic GRIP1 protein is not increased by TTX treatment, suggesting that the enhanced synaptic accumulation is attributable to a redistribution of GRIP1 rather than an increase in total protein abundance. This redistribution was transcription-dependent, suggesting that it is driven by the transcriptional up-regulation of unidentified factors during activity blockade.

In addition to playing a critical role in synaptic scaling, there is much accumulating evidence that GRIP1 is important for the expression of a Hebbian form of synaptic plasticity, LTD. The GluA2 S880E mutant has previously been shown to occlude LTD in the cerebellum by triggering PICK1-dependent AMPA receptor endocytosis (41, 48), and cerebellar LTD is blocked in a GRIP1/2 knockout (34). Given that GRIP1 and GRIP2 are able to compensate for one another in cerebellar LTD (34), it is perhaps surprising that we are able to block scaling up by KD of GRIP1 alone. These data show that GRIP1 and GRIP2 do not play entirely redundant roles in synaptic plasticity, with GRIP2 able to sustain LTD, but not synaptic scaling up, in the absence of GRIP1.

Although a number of proteins and signaling pathways have been identified that play a role in synaptic scaling, the crucial factors that lead to enhanced AMPAR accumulation during scaling up have remained obscure. Furthermore, our understanding of the function of synaptic scaling has been limited by our inability to selectively interfere with synaptic scaling while leaving baseline transmission and other forms of plasticity intact (49). Here, we show that regulated synaptic GRIP1 accumulation is necessary to induce scaling up, and we provide compelling evidence that the interaction between GluA2 and GRIP1 is critical for this process. Our data support a model of synaptic scaling in which chronic activity deprivation promotes the interaction between GluA2 and GRIP1, the trafficking of GRIP1 to synapses, and thus the GRIP1-dependent synaptic trafficking and/or stabilization of GluA2-containing AMPARs.

Experimental Procedures

Neuronal Cultures, Transfections, and Drug Treatments. Dissociated cultures were prepared from the visual cortex of postnatal day 1 (P1)–P3 Long–Evans rats and plated onto glass-bottomed dishes as described previously (50). All experiments were performed after 7–10 DIV. Neurons were transfected at low efficiency with Lipofectamine 2000 2 d before recording or immunostaining, unless otherwise noted. To visualize transfected neurons, constructs were cotransfected with cyanofluorescent protein (CFP). To induce synaptic scaling, neurons were treated with 5 μM TTX for 6 h. For ActD treatment, cultures were treated with 50 μM ActD (Sigma-Aldrich; A 1410) ± TTX for 6 h; ActD was dissolved in DMSO, with the final concentration of DMSO at

1:1,000; control cultures were treated with DMSO only. For all experiments, matched controls from sister cultures were obtained for each experimental condition. There were no significant differences in control mEPSC amplitude between different experiments (ANOVA, $P = 0.56$), so control values were pooled in Figs. 4 and 6. Unless stated otherwise, data are presented as the means ± SEM for the number of neurons indicated; where data are presented as percentage of control values, the propagated SEM was used.

Construct Design. The GluA2 shRNA and RNAiI GluA2 were designed as described in ref. 12. Site-directed mutagenesis was used to create the RNAiI GluA2 C-tail mutants. The presence of mutations was verified with sequencing. The GRIP1 shRNA and GRIP1 rescue construct were gifts from Casper Hoogenraad, Utrecht University, Utrecht, The Netherlands.

Immunocytochemistry. Permeabilized immunostaining was performed as described (51) using antibodies against the following: PSD-95 (1:200; MA1-046, Thermo Scientific); synapsin 1 and 2 (1:1,000, 106 004, Synaptic Systems); GRIP1 [1:800, ab25963, Abcam; or 1:400, Mouse (Ms) Anti-GRIP1, 611319, BD Transduction Laboratories]; and Sec8 (1:450, 610659; BD Transduction Laboratories). To visualize surface GluA2 (1:50, MAB397, Chemicon; ms monoclonal antibody, gift of Eric Gouaux, Vollum Institute, Oregon Health & Science University, Portland, Oregon) and GFP (1:100, AB3080P; Millipore), live neurons were incubated with antibodies under nonpermeable conditions as described in ref. 11. Alexa Fluor 488, Texas red, and Alexa Fluor 657 (1:200; Invitrogen) were used as secondary antibodies. Digital images were acquired with Openlab (Improvision) or Volocity (PerkinElmer) software on an Olympus IX-81 microscope with an oil immersion 60× objective using an Orca ER camera. A 6% neutral density filter was used during image acquisition to prevent photobleaching. Digital images were quantified with Metamorph software (Molecular Devices). Localization of GRIP1 to recycling endosome and Sec8-labeled compartments was performed with LSM5 Leica confocal microscope under sequential scanning settings for multichannel fluorescence image acquisition. To ensure uniformity, data were acquired from the apical-like dendrite and dendritic branches off of it. Puncta were selected by thresholding above local background with the Granularity function in Metamorph. Experimental conditions were run in parallel with the control condition on sister cultures from the same dissociations; the mean total puncta intensity for experimental conditions was normalized to the mean total puncta intensity of control in sister cultures. Similar results were obtained when average puncta intensity was used.

Because the Sec8 puncta density was high, we wished to verify that the colocalization we observed between Sec8 and GRIP1 puncta was greater than expected for random colocalization of the two signals. To estimate the expected random colocalization rate, we generated artificial Sec8 images in ImageJ using the ThunderSTORM plugin. An Integrated gaussian option was used to generate artificial puncta with a similar size and intensity distribution to the Sec8 images (full width at half maximum range from 200 to 350 nm, intensity range from 700 to 900 photons). Average Sec8 puncta density values obtained from Sec8 experimental images were then used to create an artificial Sec8 image, by randomly distributing these artificial puncta at the experimental density measured for each image pair, and the colocalization rate was determined using the same criteria as for the experimental images. This "random" rate was then compared with the experimentally measured rate for each image pair.

Transferrin Labeling. To label recycling endosomes, cells were incubated with 50 ng/μL Alexa Fluor 546-labeled transferrin in neuronal culture media for 30 min at 37 °C in the incubator. After incubation, cells were removed from the incubator and washed three times in phosphate buffered saline (PB) followed by fixation with 3.7% (wt/vol) paraformaldehyde in PB. Cells were then permeabilized and stained using various antibodies as described (51).

Immunoelectron Microscopy. Neurons were plated on gridded coverslips under normal culture conditions (catalog no. P35G-2-14-GCRD; Matek); 7- to 9-DIV pyramidal neurons were identified based on morphology and their location on the dish was noted. Cells were fixed in 4% paraformaldehyde, labeled with guinea pig anti-VGluT1 antibody (1:600, catalog no. 135 304; Synaptic Systems) followed by biotinylated anti-guinea pig secondary antibody (1:400, catalog no. BA-7000; Vector Labs) and then immersed in a 1% DAB solution in the presence of H_2O_2 solution for 1–2 min. Next neurons were dehydrated through a series of ethanol and acetone mixtures. After dehydration, a BEEM capsule was placed over the region of interest, filled with EPON resin (catalog no. 14120; EMS), and placed in a 60 °C oven to polymerize. After polymerization, blocks containing pyramidal neurons were quickly immersed in liquid N_2 to remove the EPON block from the culture dish. Blocks were then trimmed, imaged on a dissection scope to correlate with imaging on the electron microscope, and sectioned on an ultramicrotome to 50- to 70-nm thickness. Ultrathin sections containing identified pyramidal neurons were placed on nickel formvar-coated slot grids and sections were postembedding labeled with a rabbit anti-GRIP1 antibody (1:200; ab25963, Abcam), followed by anti-rabbit 5-nm gold-conjugated secondary antibody (1:25; catalog no. 15725; Ted Pella). Identified pyramidal neurons were relocated under electron microscopy and examined for the presence of VGluT1 DAB-labeled presynaptic boutons forming synapses onto pyramidal spines, dendrites, or somata. DAB-labeled synapses were deemed "VGluT1-positive" if they contained at least 3 DAB-labeled presynaptic vesicles, had parallel alignment of pre- and postsynaptic membranes, and contained a postsynaptic density. VGluT1-positive synapses were imaged at 16,000× to 20,000× magnification, corresponding to a pixel size of 1.4–0.9 nm, respectively. Captured images of positive synapses were analyzed for the distribution and density of GRIP1-gold particles. The centroid and edges of the postsynaptic density were used to define the midpoint and lateral edges of synapses, and the centroid of the synaptic cleft was defined as the midpoint for axospinous/dendritic distribution measurements. Grip1-gold particle density was calculated as: number of gold particles within 40-nm radius of the synaptic cleft centroid/synapse length (as defined by the postsynaptic density). Statistical significance was determined with Mann–Whitney U test with significance set at $P < 0.05$.

Electrophysiology. Whole-cell AMPA-mediated mEPSC recordings were obtained and analyzed as described previously (4, 11) from visually identified pyramidal neurons at 25 °C from a holding potential of −70 mV in the following artificial CSF (ACSF): 126 mM NaCl, 5.5 mM KCl, 2 mM $MgSO_4$, 1 mM NaH_2PO_4, 25 mM $NaHCO_3$, 2 mM $CaCl_2$, 14 mM dextrose, 0.1 μM TTX, 0.025 mM picrotoxin, and 0.025 mM D-amino-5-phosphovaleric acid. The internal recording solution contained the following (in mM): 120 $KMeSO_4$, 10 KCl, 2 $MgSO_4$, 10 K-Hepes, 0.5 EGTA, 3 K_2ATP, 0.3 NaGTP, and 10 Na_2 phosphocreatine. Recordings with resting membrane potential (V_m) greater than −55 mV, series resistance (R_s) >20 MΩ, input resistance (R_{in}) <150 MΩ, a change in R_{in} or V_m >30%, or <25 mEPSCs were excluded. Cumulative amplitude histograms of mEPSC amplitude were created using the first 25 events from each neuron, as described (4).

Statistical Analysis. Data are reported as means ± SEM for the number of neurons indicated. Unless otherwise indicated, statistical tests were two-tailed Student t tests or, for multiple comparisons, single-factor ANOVAs followed by two-tailed Student t tests or post hoc Tukey tests.

ACKNOWLEDGMENTS. We thank Lirong Wang for technical assistance, Geoff Hahn for generating the images in Fig. S1, Casper Hoogenraad for kindly providing the GRIP1 shRNA and rescue constructs, Eric Gouaux for the gift of the GluA2 antibody, and Jennifer Wolff for help designing the GluA2 mutants. This research was supported by National Institutes of Health Grants R01NS036853/NS092635 (to G.G.T.) and F31NS063532 (to M.A.G.).

1. Abbott LF, Nelson SB (2000) Synaptic plasticity: Taming the beast. *Nat Neurosci* 3 (Suppl):1178–1183.
2. Pozo K, Goda Y (2010) Unraveling mechanisms of homeostatic synaptic plasticity. *Neuron* 66(3):337–351.
3. Turrigiano GG, Nelson SB (2004) Homeostatic plasticity in the developing nervous system. *Nat Rev Neurosci* 5(2):97–107.
4. Turrigiano GG, Leslie KR, Desai NS, Rutherford LC, Nelson SB (1998) Activity-dependent scaling of quantal amplitude in neocortical neurons. *Nature* 391(6670): 892–896.
5. Ibata K, Sun Q, Turrigiano GG (2008) Rapid synaptic scaling induced by changes in postsynaptic firing. *Neuron* 57(6):819–826.
6. Goold CP, Nicoll RA (2010) Single-cell optogenetic excitation drives homeostatic synaptic depression. *Neuron* 68(3):512–528.
7. Pratt KG, Zimmerman EC, Cook DG, Sullivan JM (2011) Presenilin 1 regulates homeostatic synaptic scaling through Akt signaling. *Nat Neurosci* 14(9):1112–1114.
8. Trasande CA, Ramirez JM (2007) Activity deprivation leads to seizures in hippocampal slice cultures: Is epilepsy the consequence of homeostatic plasticity? *J Clin Neurophysiol* 24(2):154–164.
9. Anggono V, Huganir RL (2012) Regulation of AMPA receptor trafficking and synaptic plasticity. *Curr Opin Neurobiol* 22(3):461–469.
10. O'Brien RJ, et al. (1998) Activity-dependent modulation of synaptic AMPA receptor accumulation. *Neuron* 21(5):1067–1078.
11. Wierenga CJ, Ibata K, Turrigiano GG (2005) Postsynaptic expression of homeostatic plasticity at neocortical synapses. *J Neurosci* 25(11):2895–2905.
12. Gainey MA, Hurvitz-Wolff JR, Lambo ME, Turrigiano GG (2009) Synaptic scaling requires the GluR2 subunit of the AMPA receptor. *J Neurosci* 29(20):6479–6489.

13. Diering GH, Gustina AS, Huganir RL (2014) PKA-GluA1 coupling via AKAP5 controls AMPA receptor phosphorylation and cell-surface targeting during bidirectional homeostatic plasticity. *Neuron* 84(4):790–805.
14. Altimimi HF, Stellwagen D (2013) Persistent synaptic scaling independent of AMPA receptor subunit composition. *J Neurosci* 33(29):11763–11767.
15. Dong H, et al. (1997) GRIP: A synaptic PDZ domain-containing protein that interacts with AMPA receptors. *Nature* 386(6622):279–284.
16. Dev KK, Nishimune A, Henley JM, Nakanishi S (1999) The protein kinase C alpha binding protein PICK1 interacts with short but not long form alternative splice variants of AMPA receptor subunits. *Neuropharmacology* 38(5):635–644.
17. Osten P, et al. (2000) Mutagenesis reveals a role for ABP/GRIP binding to GluR2 in synaptic surface accumulation of the AMPA receptor. *Neuron* 27(2):313–325.
18. Daw MI, et al. (2000) PDZ proteins interacting with C-terminal GluR2/3 are involved in a PKC-dependent regulation of AMPA receptors at hippocampal synapses. *Neuron* 28(3):873–886.
19. Braithwaite SP, Xia H, Malenka RC (2002) Differential roles for NSF and GRIP/ABP in AMPA receptor cycling. *Proc Natl Acad Sci USA* 99(10):7096–7101.
20. Lin DT, Huganir RL (2007) PICK1 and phosphorylation of the glutamate receptor 2 (GluR2) AMPA receptor subunit regulates GluR2 recycling after NMDA receptor-induced internalization. *J Neurosci* 27(50):13903–13908.
21. Mejias R, et al. (2011) Gain-of-function glutamate receptor interacting protein 1 variants alter GluA2 recycling and surface distribution in patients with autism. *Proc Natl Acad Sci USA* 108(12):4920–4925.
22. Mao L, Takamiya K, Thomas G, Lin DT, Huganir RL (2010) GRIP1 and 2 regulate activity-dependent AMPA receptor recycling via exocyst complex interactions. *Proc Natl Acad Sci USA* 107(44):19038–19043.
23. Anggono V, Clem RL, Huganir RL (2011) PICK1 loss of function occludes homeostatic synaptic scaling. *J Neurosci* 31(6):2188–2196.
24. Dong H, et al. (1999) Characterization of the glutamate receptor-interacting proteins GRIP1 and GRIP2. *J Neurosci* 19(16):6930–6941.
25. Srivastava S, Ziff EB (1999) ABP: A novel AMPA receptor binding protein. *Ann N Y Acad Sci* 868:561–564.
26. Torres R, et al. (1998) PDZ proteins bind, cluster, and synaptically colocalize with Eph receptors and their ephrin ligands. *Neuron* 21(6):1453–1463.
27. Ye B, et al. (2000) GRASP-1: A neuronal RasGEF associated with the AMPA receptor/GRIP complex. *Neuron* 26(3):603–617.
28. Wyszynski M, et al. (2002) Interaction between GRIP and liprin-alpha/SYD2 is required for AMPA receptor targeting. *Neuron* 34(1):39–52.
29. Setou M, et al. (2002) Glutamate-receptor-interacting protein GRIP1 directly steers kinesin to dendrites. *Nature* 417(6884):83–87.
30. Steiner P, et al. (2005) Interactions between NEEP21, GRIP1 and GluR2 regulate sorting and recycling of the glutamate receptor subunit GluR2. *EMBO J* 24(16):2873–2884.
31. Kulangara K, et al. (2007) Phosphorylation of glutamate receptor interacting protein 1 regulates surface expression of glutamate receptors. *J Biol Chem* 282(4):2395–2404.
32. Chung HJ, Xia J, Scannevin RH, Zhang X, Huganir RL (2000) Phosphorylation of the AMPA receptor subunit GluR2 differentially regulates its interaction with PDZ domain-containing proteins. *J Neurosci* 20(19):7258–7267.
33. Xia J, Chung HJ, Wihler C, Huganir RL, Linden DJ (2000) Cerebellar long-term depression requires PKC-regulated interactions between GluR2/3 and PDZ domain-containing proteins. *Neuron* 28(2):499–510.
34. Takamiya K, Mao L, Huganir RL, Linden DJ (2008) The glutamate receptor-interacting protein family of GluR2-binding proteins is required for long-term synaptic depression expression in cerebellar Purkinje cells. *J Neurosci* 28(22):5752–5755.
35. Steinmetz CC, Turrigiano GG (2010) Tumor necrosis factor-α signaling maintains the ability of cortical synapses to express synaptic scaling. *J Neurosci* 30(44):14685–14690.
36. Watt AJ, van Rossum MC, MacLeod KM, Nelson SB, Turrigiano GG (2000) Activity coregulates quantal AMPA and NMDA currents at neocortical synapses. *Neuron* 26(3):659–670.
37. Wyszynski M, et al. (1999) Association of AMPA receptors with a subset of glutamate receptor-interacting protein in vivo. *J Neurosci* 19(15):6528–6537.
38. Bladt F, Tafuri A, Gelkop S, Langille L, Pawson T (2002) Epidermolysis bullosa and embryonic lethality in mice lacking the multi-PDZ domain protein GRIP1. *Proc Natl Acad Sci USA* 99(10):6816–6821.
39. Takamiya K, et al. (2004) A direct functional link between the multi-PDZ domain protein GRIP1 and the Fraser syndrome protein Fras1. *Nat Genet* 36(2):172–177.
40. Hoogenraad CC, Milstein AD, Ethell IM, Henkemeyer M, Sheng M (2005) GRIP1 controls dendrite morphogenesis by regulating EphB receptor trafficking. *Nat Neurosci* 8(7):906–915.
41. Chung HJ, Steinberg JP, Huganir RL, Linden DJ (2003) Requirement of AMPA receptor GluR2 phosphorylation for cerebellar long-term depression. *Science* 300(5626):1751–1755.
42. Matsuda S, Mikawa S, Hirai H (1999) Phosphorylation of serine-880 in GluR2 by protein kinase C prevents its C terminus from binding with glutamate receptor-interacting protein. *J Neurochem* 73(4):1765–1768.
43. Hayashi T, Huganir RL (2004) Tyrosine phosphorylation and regulation of the AMPA receptor by SRC family tyrosine kinases. *J Neurosci* 24(27):6152–6160.
44. Seidenman KJ, Steinberg JP, Huganir R, Malinow R (2003) Glutamate receptor subunit 2 Serine 880 phosphorylation modulates synaptic transmission and mediates plasticity in CA1 pyramidal cells. *J Neurosci* 23(27):9220–9228.
45. Perez JL, et al. (2001) PICK1 targets activated protein kinase Calpha to AMPA receptor clusters in spines of hippocampal neurons and reduces surface levels of the AMPA-type glutamate receptor subunit 2. *J Neurosci* 21(15):5417–5428.
46. Hsu SC, TerBush D, Abraham M, Guo W (2004) The exocyst complex in polarized exocytosis. *Int Rev Cytol* 233:243–265.
47. Bakshi K, et al. (2009) Prenatal cocaine reduces AMPA receptor synaptic expression through hyperphosphorylation of the synaptic anchoring protein GRIP. *J Neurosci* 29(19):6308–6319.
48. Steinberg JP, et al. (2006) Targeted in vivo mutations of the AMPA receptor subunit GluR2 and its interacting protein PICK1 eliminate cerebellar long-term depression. *Neuron* 49(6):845–860.
49. Turrigiano GG (2008) The self-tuning neuron: Synaptic scaling of excitatory synapses. *Cell* 135(3):422–435.
50. Pratt KG, Watt AJ, Griffith LC, Nelson SB, Turrigiano GG (2003) Activity-dependent remodeling of presynaptic inputs by postsynaptic expression of activated CaMKII. *Neuron* 39(2):269–281.
51. Rutherford LC, DeWan A, Lauer HM, Turrigiano GG (1997) Brain-derived neurotrophic factor mediates the activity-dependent regulation of inhibition in neocortical cultures. *J Neurosci* 17(12):4527–4535.

Supporting Information

Gainey et al. 10.1073/pnas.1510754112

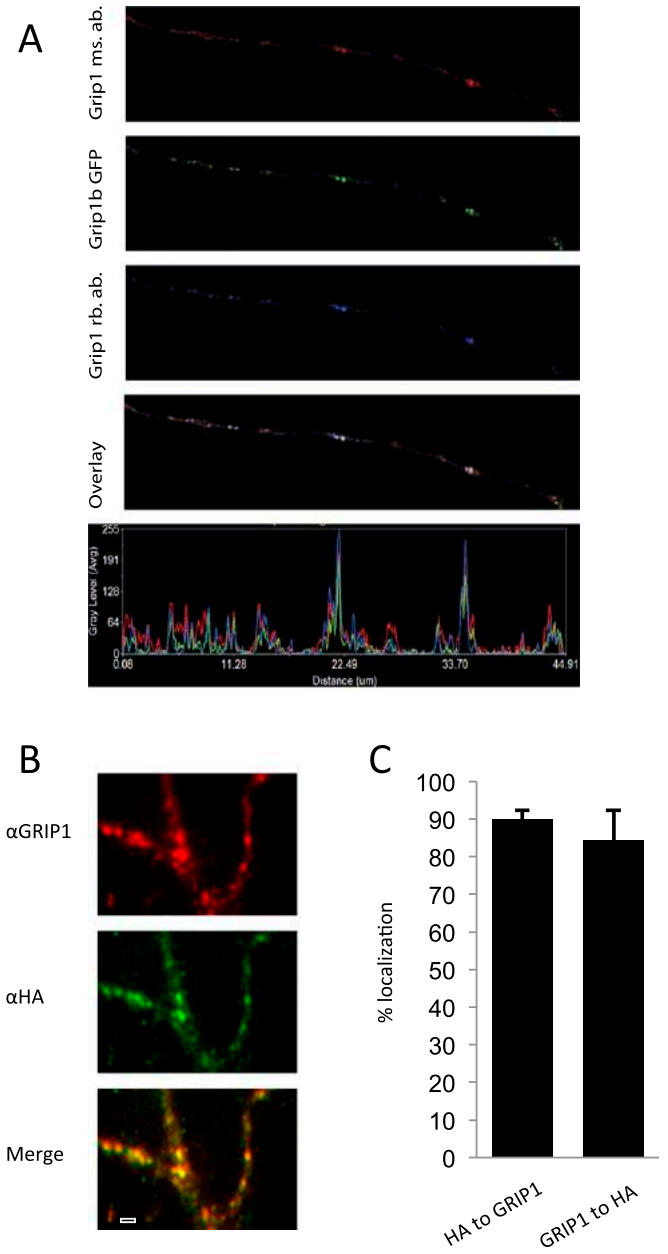

Fig. S1. Characterization of GRIP1 antibodies. (*A*) Neurons transfected with GRIP1b GFP (green) were stained with αGRIP1 Ms 611319 (BD Transduction Laboratories) (red), and αGRIP1 rb ab25963 (Abcam) (blue). The bottom graph demonstrates intensity values of all three signals from a line scan that was drawn along the dendrite. (*B* and *C*) Neurons transfected with HA-tagged GRIP1b (green) were stained with αGRIP1 antibody rb ab25963 (red) (*B*), and the colocalization rates of the two signals were determined (*C*).

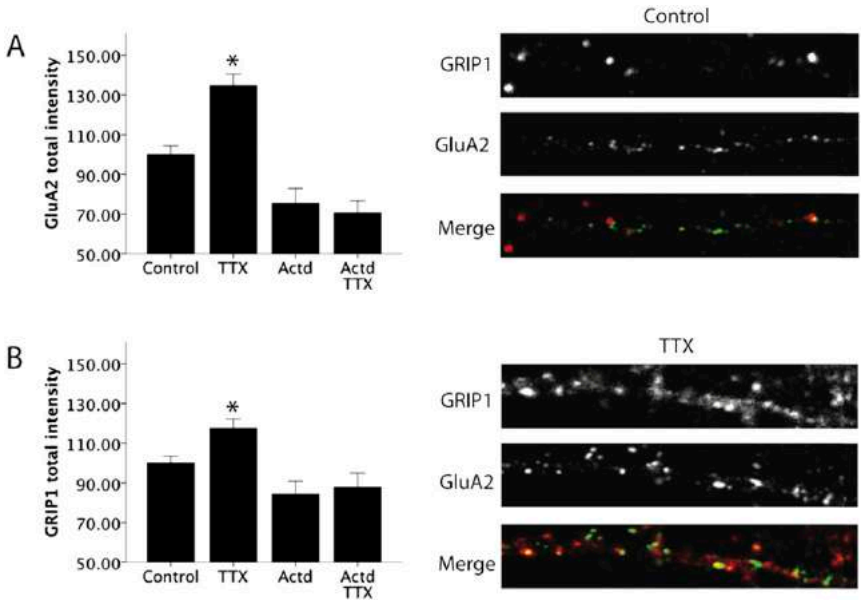

Fig. S2. The TTX-induced increase in GluA2 and GRIP1 signal at colocalized puncta is transcription-dependent. Neurons were treated with TTX for 6 h with or without ActD and then were fixed, permeabilized, and stained against GluA2 and GRIP1. At right are representative images of GRIP1/GluA2 staining for control (*Upper*) and TTX-treated (*Lower*) dendrites. (*A*) The intensity of the signal at colocalized puncta was then quantified for each condition and expressed as percentage of untreated control neurons; for GluA2 (*A*) and for GRIP1 (*B*). Control, $n = 83$ neurons; TTX, $n = 91$; neurons Act D, $n = 43$; Act D TTX, $n = 41$. (Scale bar: 1 μm.)

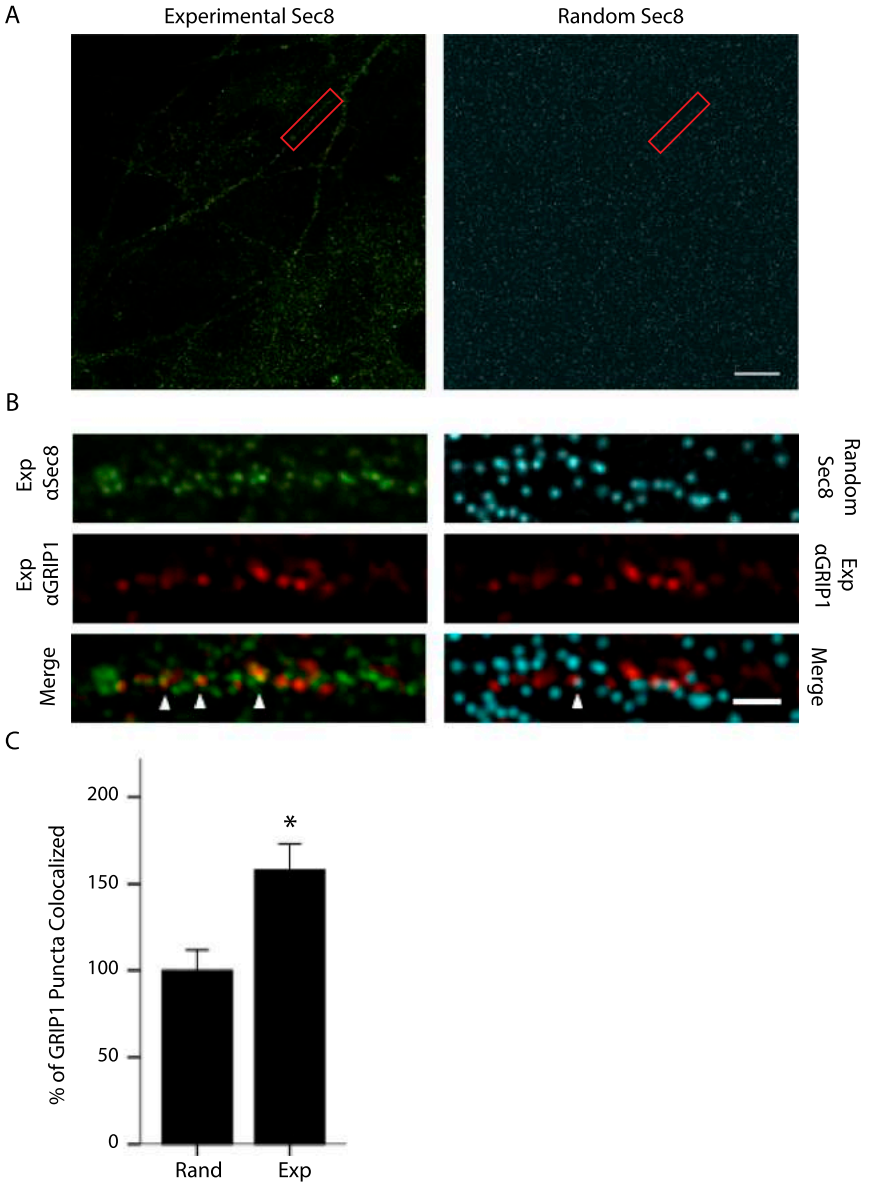

Fig. S3. Quantification of expected random colocalization rates. (*A*) Example of an experimental Sec8 image (*Left*) and an artificially generated Sec8 image (*Right*), in which puncta with the same size and intensity distribution as in the real data are randomly distributed throughout the field of view. Red box designates inset for *B*. (Scale bar: 10 μm.) (*B*, *Left*) Representative images for Sec8 (green) and GRIP1 (red) staining, with the merge shown below. (*B*, *Right*) Artificially generated Sec8 image (blue) and real GRIP1 image (red), with merge shown below. Arrows mark sites of colocalization. (Scale bar: 2 μm.) (*C*) Percentage of GRIP1 puncta that were colocalized with Sec8 in the random and experimental conditions ($n = 71$ images). *Experiment different from random, $P < 0.05$.

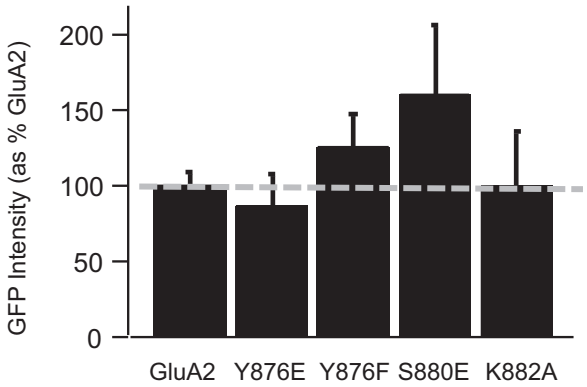

Fig. S4. Quantification of the synaptic surface expression of various GluA2 mutants. Receptors were N-terminal–tagged with GFP, and surface GFP fluorescence was detected using a GFP antibody under nonpermeant conditions. The intensity of the GFP signal at puncta colocalized with PSD-95 was determined. There were no significant differences across mutants (ANOVA) (n = 6 neurons per condition).